Hindawi
Adsorption Science & Technology
Volume 2021, Article ID 4158151, 14 pages
https://doi.org/10.1155/2021/4158151

Research Article

Experimental Study of the Adsorption of Nitrogen and Phosphorus by Natural Clay Minerals

Tingyu Fan,[1,2,3] Miao Wang,[1,3] Xingming Wang,[2] Yingxiang Chen,[1,3] Shun Wang,[1,3] Hongbin Zhan,[4] Xiaoyang Chen,[1,3] Akang Lu,[1,3] and Shijiao Zha[1,3]

[1]*School of Earth and Environment, Anhui University of Science and Technology, Huainan 232001, China*
[2]*State Key Laboratory of Simulation and Regulation of Water Cycle in River Basin, China Institute of Water Resources and Hydropower Research, Beijing 100038, China*
[3]*Anhui Engineering Laboratory for Comprehensive Utilization of Water and Soil Resources & Ecological Protection in Mining Area with High Groundwater Level, Huainan 232001, China*
[4]*Department of Geology and Geophysics, Texas A&M University, College Station, TX 77843-3115, USA*

Correspondence should be addressed to Xingming Wang; xmwang-2004@126.com

Received 8 June 2021; Revised 22 September 2021; Accepted 5 October 2021; Published 5 November 2021

Academic Editor: Huihui Du

Nitrogen and phosphorus are commonly recognized as causing eutrophication in aquatic systems, and their transport in subsurface environments has also aroused great public attention. This research presented four natural clay minerals (NCMs) evaluated for their effectiveness of NH_4^+ and PO_4^{3-} adsorption from wastewater. All the NCMs were fully characterized by X-ray diffraction (XRD), Fourier transform infrared spectroscopy (FTIR), scanning electron microscopy (SEM), BET analysis, and adsorption kinetics and isotherms to better understand the adsorption mechanism-property relationship. The results show that the adsorption efficiency of the four NCMs for phosphate was better than that for ammonia nitrogen. The removal rate of phosphate was higher than 65%, generally in the range of 80%-90%, while the removal rate of ammonia nitrogen was less than 50%. The adsorption kinetic behavior followed the pseudo-second-order kinetic model. The ammonia nitrogen adsorption isotherm was in good agreement with the Freundlich isotherm equilibrium model, and the phosphate adsorption isotherm matched the Langmuir model. Among all the NCMs studied, bentonite (7.13 mg/g) and kaolinite (5.37 mg/g) showed higher adsorption capacities for ammonia nitrogen, while zeolite (0.21 mg/g) and attapulgite (0.17 mg/g) showed higher adsorption capacities for phosphate. This study provides crucial baseline knowledge for the adsorption of nitrogen and phosphate by different kinds of NCMs.

1. Introduction

With the development of human society, the impacts on water quality from industrial and human activity continue to increase [1, 2]. Industrial wastewater and domestic sewage containing nitrogen and phosphorus are still often directly discharged into natural water bodies without effective treatment [3, 4]. Natural reservoirs, lakes, and oceans are facing severe water eutrophication problems [5, 6]. In particular, the high concentration of nitrogen and phosphorus in natural water bodies is the main cause of eutrophication of water bodies [7–10]. How to deal with nitrogen- and phosphorus-polluted water has become a matter of widespread concern.

For the removal of excess nitrogen and phosphorus in eutrophic water bodies, many methods have been developed over several decades of investigations, including physical treatment and chemical treatment, biodegradation, and selective ion exchange [11–14]. For practical applications, adsorption is the most advantageous remediation method due to its low cost, small energy consumption, and relative ease in implementation [15, 16]. Among various adsorbents, clay minerals are highly favorable due to their advantages of easy availability, low cost, and lack of secondary contamination to the ecological environment, and they are key components of soil [6, 17–19]. Four representative minerals including kaolinite, zeolite, attapulgite, and bentonite could

be commonly found in soil and sediments. These minerals have good ion exchange capacity and exhibit a certain adsorption effect on pollutants in water or soil, especially on nutrients such as nitrate, ammonia, and phosphate [20, 21]. Clay minerals are the most important adsorbents which have made a significant contribution to the natural self-purification capacity of water and soil environments.

Many scholars focus on the clay mineral's adsorption property for treating nitrogen and phosphorus compounds, such as nitrate in groundwater and ammonia in surface water, wastewater, or soil [22–26]. For example, natural zeolite has been used to remediate the sediments in eutrophic lakes because it has a high ion exchange capacity and high selectivity for NH_4^+ [27]. It is proved to be feasible to use bentonite, illite, and zeolite as capping materials to stabilize nutrients and interrupt their release from contaminated lake sediments. Bentonite was especially used to capture phosphate released from sediments [28].

Several factors such as concentration, pH, and temperature could affect the adsorption behavior, especially the concentration of raw water. We could divide the nitrogen or phosphorus concentration of raw water into three types: high level (hundreds of mg/L), medium level (dozens of mg/L), and low level (a fraction of mg/L). For instance, the PO_4^{3-} adsorption capacity of TiO_2/Yemeni natural zeolite may reach 37.6 mg/g from the raw water of 80 mg/L phosphate, and the Freundlich model provided the best fit for the equilibrium data [29]. For eutrophic water with 0.1 mg/L phosphate and 2 mg/L ammonia nitrogen, one novel bentonite-humic acid composite Bephos™ could show phosphate adsorption capacities of 26.5 mg/g and ammonia nitrogen adsorption capacities of 202.1 mg/g, respectively. The Langmuir and Freundlich models both fitted well with the experimental results, and the pseudo-second-order kinetic model correlated well with the experimental results [30]. The ammonia nitrogen adsorption of halloysite was saturated with 1.66 mg/g at 303 K, pH of 5.6 in 600 mg/L solution ammonia nitrogen, and the ammonia nitrogen isothermal adsorption of halloysite matched the Langmuir and Freundlich isotherms, and the adsorption process conformed closely to the pseudo-second-order kinetic equation [31].

A previous study mainly adopted modified clay minerals to maximize their adsorption capacity for nutrients. Although a relatively high treatment effect could be achieved, modified clay minerals or materials were commonly applied in the lab or small-scale application, but they were expensive and infeasible to mass production and large-scale use to treat nutrients in natural eutrophic lakes. By comparison, the adsorption behavior of natural clay minerals would have more practical applications, especially for eutrophic water bodies with slightly higher nitrogen of 0.2–0.3 mg/L and phosphorus concentrations of 0.01–0.02 mg/L. Moreover, most existing research studies were independent [32]. There was a lack of systematic and comprehensive comparative studies under the same conditions. Therefore, we focused on the natural clay minerals and chose eutrophic waters with slightly higher nitrogen and phosphorus concentrations, which helped us to understand the structure and properties of NCMs and their adsorption effects on NH_4^+ and PO_4^{3-}.

This study evaluated four common natural clay minerals, namely, kaolinite, zeolite, attapulgite, and bentonite, as adsorbents under the same experimental conditions, and studied the adsorption behavior of ammonium ions and phosphate on the surface of NCMs. We made a comprehensive comparison of adsorption capacities, adsorption kinetics, adsorption isotherms, and different influencing factors such as pH, adsorbent dose, and temperature. The NCM samples before and after adsorption were characterized by XRD, FTIR, SEM, and BET analysis to determine the mineralogical properties. This research could provide meaningful references for the exploration of the self-purification function of NCMs.

2. Materials and Methods

2.1. Characterization of Natural Clay Minerals. Kaolinite, zeolite, attapulgite, and bentonite were the tested adsorbents in this paper. They were purchased from Gongyi City Yuan-Xiang Water Purification Materials Factory (China). All natural clay minerals are in powder form and in grey. They are aluminosilicate minerals, with cavities and pores with a certain pore size, and have good adsorption and ion exchange properties.

The surface elemental composition of NCMs was determined by XRD (SmartLab SE, Science, Japan). The SEM (FlexSEM 1000, Hitachi, Japan) was used to examine the morphology of NCMs. The functional groups of NCMs were analyzed by FTIR (Nicolet iS50, Thermo Fisher Scientific, USA). The specific surface area was measured by BET analysis (ASAP 2460 3.01, Micromeritics, USA).

The XRD crystallinity of four NCMs was calculated based on the percentage of the contribution of the crystal region in the total area of the XRD intensity peak of the clay mineral. The four NCMs in the samples were identified using the MDI Jade software package (version 6.5).

2.2. Batch Adsorption Experiments. To simulate a water body with a high degree of eutrophication, the concentrations of ammonia nitrogen and phosphate in the experiment were selected to be 20 mg/L and 10 mg/L, respectively.

The adsorption isotherm was determined by using 25 milliliters of phosphate aqueous solutions with different initial concentrations (from 1 to 50 mg/L) and 0.3 g of the sample. The experiment was performed at room temperature (25 ± 1°C, pH 7), the suspension was separated by centrifugation, and the concentration in the supernatant was measured by molybdate spectrophotometry.

The adsorption isotherm was determined by batching 25 milliliters of ammonium chloride solutions with different initial concentrations (from 5 to 100 mg/L) and 0.3 g of the sample. The experiment was carried out at room temperature (25 ± 1°C, pH 7), the suspension was separated by centrifugation, and the concentration in the supernatant was measured by Nessler's reagent spectrophotometry. A blank sample without any adsorbent was used as a control for testing.

The adsorption kinetic data of phosphate and ammonia nitrogen on natural clay minerals at contact times of 5 to

240 min were studied. The experimental conditions were as follows: pH 7, phosphate concentration 10 mg/L, ammonia nitrogen concentration 20 mg/L, adsorbent dosage 0.3 g, and temperature 25 ± 1°C.

To investigate the effect of pH on adsorption, adsorption experiments were carried out at pH 2, 4, 6, 8, and 10. The other conditions were as follows: phosphate concentration 10 mg/L, ammonia nitrogen concentration 20 mg/L, adsorbent dosage 0.3 g, and temperature 25 ± 1°C.

Experiments were also set up with distinct adsorptive doses, weighing 0.1 g, 0.2 g, 0.3 g, 0.4 g, and 0.5 g of natural clay minerals for ammonia nitrogen and phosphate adsorption experiments, with the following experimental conditions: pH 7, phosphate concentration 10 mg/L, ammonia nitrogen concentration 20 mg/L, and temperature 25 ± 1°C.

To evaluate the effects of different temperatures, batch experiments were performed at 25, 35, 45, and 55°C. The experiment was performed in a temperature-controlled water bath shaker to determine the absorption of phosphate and ammonia nitrogen at different temperatures at 25 ± 1°C, pH 7, for 24 hours [30].

2.3. Data Analyses. The removal efficiency (%) and adsorption capacity (q_e) values of adsorbed ammonium and phosphate were calculated from the concentration difference between the initial concentration (C_0) and the equilibrium concentration (C) [33].

$$\eta = \frac{C_{0-}C}{C_0} \times 100\%,$$
$$q_e = \frac{(C_0 - C)V}{M}, \quad (1)$$

where η (%) is the removal rate of ammonium or phosphate, C_0 (mg/L) is the concentration of ammonium or phosphate solution before the reaction, C (mg/L) is the concentration of ammonium or phosphate solution after the reaction, q_e (mg/g) is the adsorption capacity of ammonium nitrogen or phosphate by the adsorbent, and V (L) and M (g) are the solution volume and mass of the adsorbent [34].

To evaluate the adsorption mechanism of ammonium and phosphate, four linear models of the pseudo-first-order kinetic model, the pseudo-second-order kinetic model, the Elovich model, and the intraparticle diffusion model were adopted [35–38].

$$\text{Pseudo-first-order model}: \ln\ (q_e - q_t) = \ln q_e - K_1 t,$$
$$\text{Pseudo-second-order model}: \frac{t}{q_t} = \frac{1}{K_2 {q_e}^2} + \frac{t}{q_e},$$
$$\text{Elovich model}: q_t = \frac{1}{a} \ln (ab) + \frac{1}{a} \ln t,$$
$$\text{Intraparticle diffusion model}: q_t = c + t^{0.5} K_{td}, \quad (2)$$

where q_e and q_t are the adsorption capacities of ammonia nitrogen and phosphate (mg/g) under equilibrium and appropriate time intervals, respectively, and K_1, K_2, and K_{td} are constants of the equilibrium rate. The parameters a and b from the slope and intercept of the linearized graph, respectively, were calculated from the kinetic data.

To further analyze the adsorption mechanism, the adsorption isotherm model was introduced, including Langmuir II, Freundlich, and Temkin isotherm models [39].

$$\text{Langmuir II}: \frac{1}{q_e} = \frac{1}{bq_{max}} \left(\frac{1}{C_e}\right) + \frac{1}{q_{max}},$$
$$\text{Freundlich}: \text{Log}q_e = \frac{1}{n}\text{Log}C_e + \text{Log}K_F,$$
$$\text{Temkin}: q_e = B_T \ln A_T + B_T \ln C_e, \quad (3)$$
$$B_T = \frac{RT}{b_T}$$

where C_e is the equilibrium concentration after adsorption (mg/L), b is the Langmuir adsorption isotherm parameter (L/mg), q_e is the equilibrium adsorption capacity (mg/g), and q_{max} is the maximum adsorption capacity (mg/g). K_F and n are the Freundlich constants, which are related to the adsorptive capacity and the intensity of adsorption, T is the absolute temperature (K), R is the universal gas constant (8.314 J (mol K)$^{-1}$), B_T is the heat of adsorption, and A_T is the equilibrium binding constant (L/min), corresponding to the maximum binding energy [39].

3. Results and Discussion

3.1. Characterization

3.1.1. XRD Characterization Analysis. The XRD patterns show that the four NCMs were almost entirely composed of natural minerals and a small number of impurities, such as quartz, dolomite, and kaolinite (Figure 1(a)). Analysis showed that kaolinite contains a high content of quartz and a small amount of kaolinite; zeolite contains certain amounts of plagioclase and albite; attapulgite contains quartz and a small amount of dolomite; and bentonite contains a large amount of quartz. Therefore, the high-purity natural clay mineral sample reaches more than 90–95%, which can make an important contribution to the adsorption of nitrogen and phosphorus [40].

Among the four NCMs, kaolinite, attapulgite, and bentonite were similar in composition. They all contain quartz, and the characteristic peaks of quartz appear at 20.8°, 26.5°, and 68.8°, indicating that the three NCMs have similar properties. However, zeolite had certain differences due to its composition.

Compared with the XRD patterns before and after the adsorption of ammonia nitrogen, the characteristic peaks of the main reflection of natural clay minerals did not change greatly, and their intensity was reduced due to the adsorption of NH_4^+. This result shows that the structure of NCMs did not change much in the adsorption experiment, and most of the adsorbent was adsorbed or exchanged on

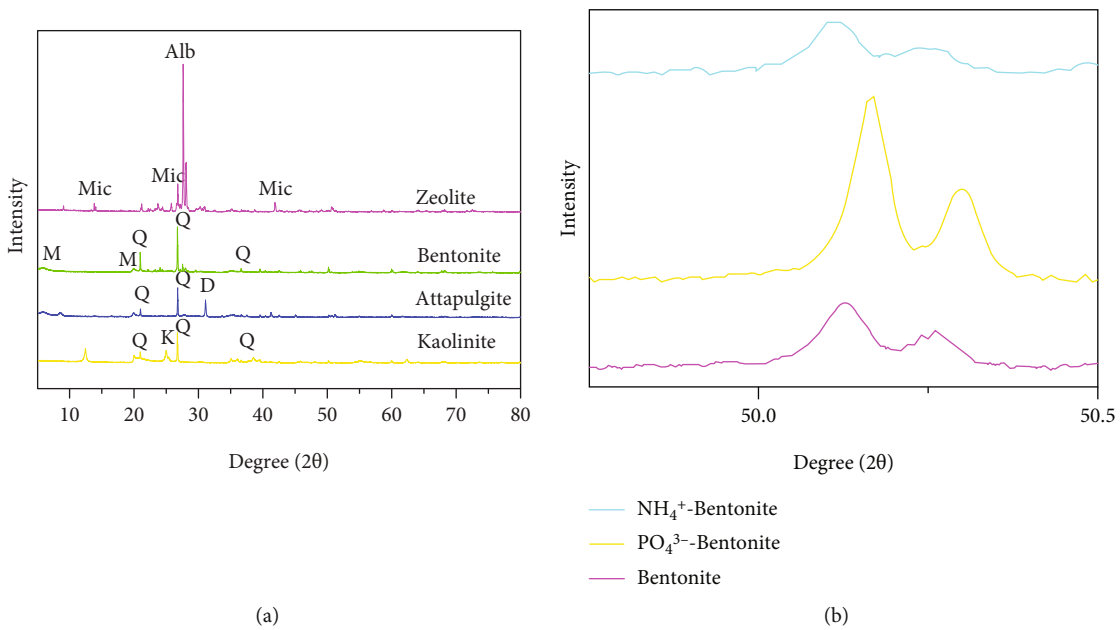

Figure 1: XRD patterns of four NCMs (a) and bentonite after adsorption of ammonia nitrogen and phosphate (b). Q = quartz; K = kaolinite; D = dolomite; Alb = albite; Mic = microcline; M = montmorillonite.

the surface of NCM particles [40]. In particular, the characteristic peak intensity of the main reflection of zeolite and attapulgite becomes weaker, while that of kaolinite is at 26.6°, and the peak intensity of bentonite at 50.2° also increases. These observations indicate that cation exchange was involved in NH_4^+ adsorption on NCM.

Compared with the XRD patterns before and after the adsorption of phosphate, the most significant change on NCM after adsorption could be observed markedly on bentonite (Figure 1(b)). The positions of main reflections of bentonite vary remarkably, which increase from 50.1 to 50.2. The significant change in interlayer distance of bentonite further confirms that more PO_4^{3-} is adsorbed [26]. The crystallinity calculation results of clay minerals after adsorbing ammonia nitrogen and phosphate changed, indicating that nitrogen and phosphorus entered the clay mineral interlayer [41]. The crystallinity of attapulgite before adsorption was 61%, and the change of crystallinity after adsorption of ammonia nitrogen and phosphate was 58% and 81%.

3.1.2. FTIR Characterization Analysis. The FTIR spectra before and after the adsorption of ammonia nitrogen and phosphate from the four natural clay minerals are shown in Figure 2. In the FTIR spectrum of kaolinite, three strong absorption peaks appeared at 3436, 3621, and 3695 cm^{-1}, which were the telescopic vibrations of hydroxyl (–OH) in kaolinite, as well as a strong absorption band at 1644 cm^{-1}, which was the absorption peak of H–OH vibrations in H–O–H in kaolinite. Peaks from 400–600 cm^{-1} belong to Si–O curved vibration absorptions, and those from 1000–1200 cm^{-1} were from Si–O telescopic vibration absorptions. After adsorption of ammonia nitrogen, the kaolinite spectrum showed signs of weakening absorptions, indicating that the kaolinite has lost part of the crystalline water, and after adsorption of phosphate, the kaolinite spectrum presented obvious signs of absorption enhancement, indicating that the kaolinite contained partially crystalline water. However, the other shapes are basically similar, indicating that the adsorption process did not change the internal structure of kaolinite [42].

In the zeolite FTIR spectrum, in the region of 400–1000 cm^{-1}, the bands correspond to the Si_2O stretching bands. The general structure of zeolite contains exchangeable cations filled between thin layers of silicate, and the composition of its basic structure indicates that zeolite has a large ion exchange performance. The band at 1672.2 cm^{-1} corresponds to single –OH stretching and bending, and the slight change suggests the involvement of hydroxyl groups in the adsorption process [43].

In the attapulgite FTIR spectrum, the typical high-frequency peaks at 3413 cm^{-1}, 3556 cm^{-1}, and 3612 cm^{-1} are caused by different types of hydroxyl telescopic vibrations in attapulgite crystals. More characteristic structural peaks of silicate minerals were observed in the low and medium frequencies. After adsorption of ammonia nitrogen and phosphate, there were obvious signs of weakening of the absorption peak of the attapulgite map features, indicating that the attapulgite participated in the adsorption reaction [44, 45].

In the bentonite FTIR spectrum, the characteristic absorption peaks of bentonite showed signs of weakening after the adsorption of ammonia nitrogen, indicating that the bentonite lost part of its crystalline water. In addition, two characteristic absorption peaks at 529 cm^{-1} and 464 cm^{-1} disappeared, which may be due to the adsorption of ammonia nitrogen. Moreover, after adsorption of phosphates, the peak intensity at 529 cm^{-1} and 464 cm^{-1} decreased, possibly as a result of interactions between phosphate root ions and hydrogen bonds and ligand exchange on bentonite [24, 46].

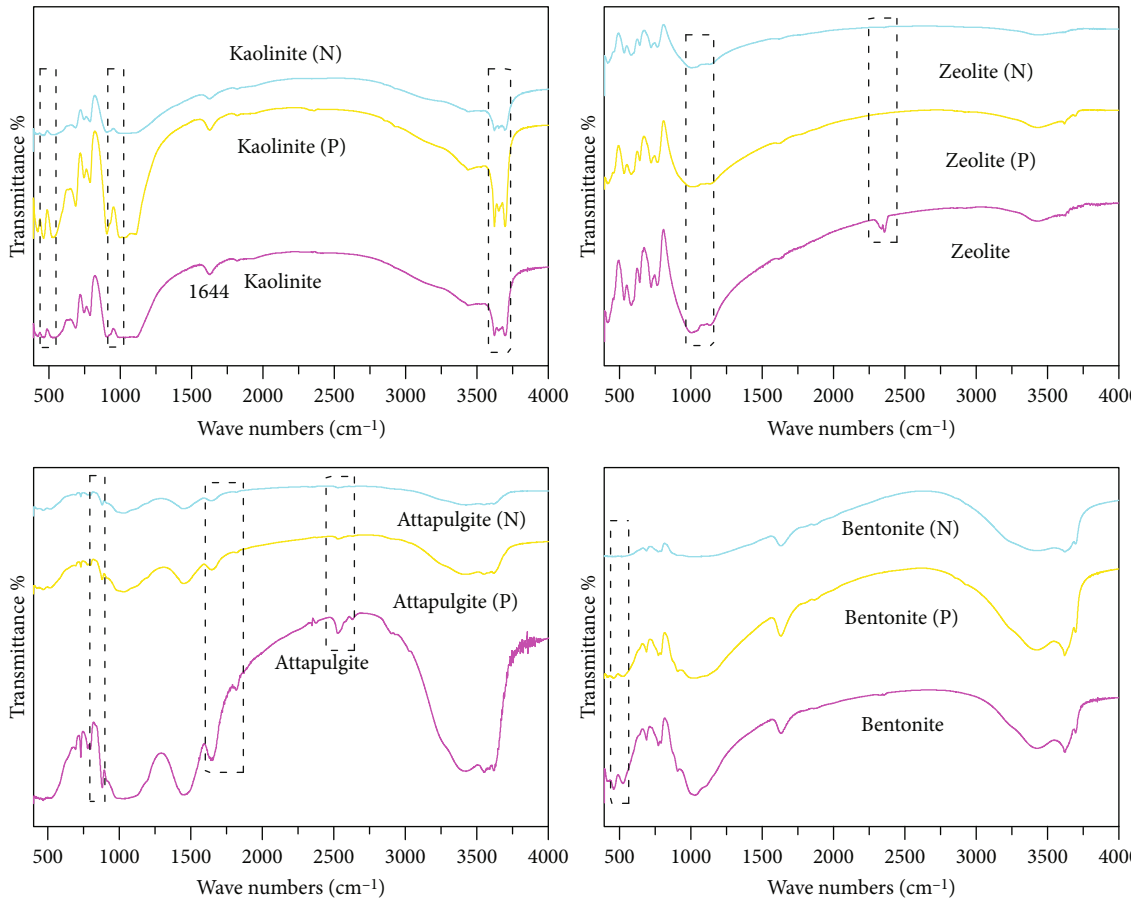

Figure 2: FTIR spectra of NCMs before and after adsorption of ammonia nitrogen (N) and phosphate (P).

3.1.3. SEM Characterization Analysis. Figure 3 shows the morphological analysis comparison diagram of kaolinite, zeolite, attapulgite, and bentonite before and after the adsorption of ammonia nitrogen and phosphate. The typical characteristic morphology of each clay mineral can be observed, namely, layered or tubular slices. The stratification and abundant folds of clay minerals are conducive to the penetration of water, enabling facile adsorption of nitrogen and phosphorus. When the aqueous solution diffuses into the clay minerals, nitrogen and phosphorus are readily captured by the active sites of the clay minerals so that the adsorption system reaches equilibrium in a short time. It can be seen from the figure that the structure of natural zeolite is tightly arranged, and the surface of the zeolite after adsorption of ammonia nitrogen is hollow, loose, and porous, with more pores extending into the interior. This result shows that the zeolite has adsorbed ammonia nitrogen. Attapulgite has a large specific surface area and a rich porous structure. Bentonite has a smooth surface and relatively small pores. Zeolite appears loose and porous, its block structure decreases, the surface is uneven and rough, and the number of pores per unit area is large [47].

The surface shape of the four clay minerals before adsorption is irregular and rough. After the adsorption of ammonia nitrogen, these materials are closely arranged and have many fine particles. This effect may be caused by the adsorption of ammonia nitrogen. Recent studies have found that the adsorption capacity of clay minerals is affected not only by their chemical location but also by their surface morphology [48]. These studies show that surface morphology plays an important role in the process of ammonia nitrogen adsorption.

After the adsorption of phosphate, due to the agglomeration of phosphate on the surface of the adsorbent, the gap between the particles is reduced, and the surface of the adsorbent becomes smooth and dense. This observation indicates that adsorption of phosphate by clay minerals has occurred.

3.1.4. BET Characterization Analysis. The N_2 adsorption/desorption isotherms and the BJH pore size distributions of attapulgite are presented in Figure 4. Its characteristic feature is a hysteresis loop, mostly attributed to mesoporous materials. From these results, the BET specific surface area, total pore volume, and average pore diameter of the attapulgite were calculated to be 92.91 m^2/g, 0.13 cm^3/g, and 5.71 nm, respectively. In addition, the BET analysis results of the other natural clay minerals are shown in Table 1. The specific surface area of attapulgite is the largest, followed by bentonite and kaolinite, and that of zeolite is the smallest [29].

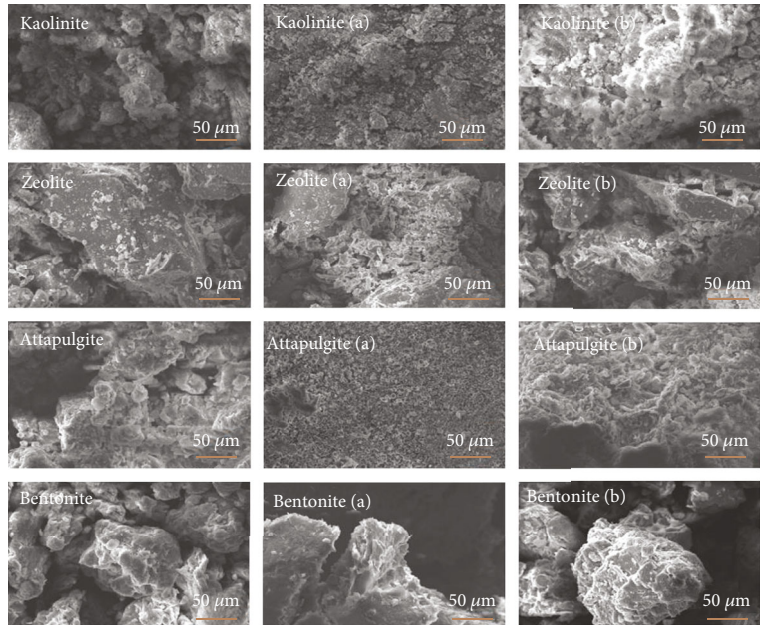

Figure 3: SEM patterns of four NCMs before and after adsorption of ammonia nitrogen (a) and phosphate (b).

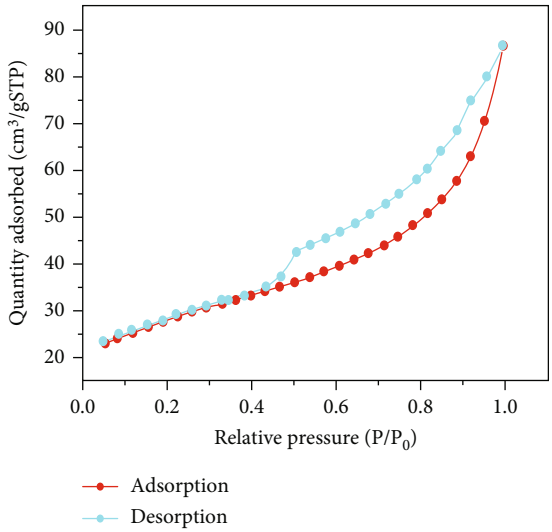

Figure 4: The adsorption/desorption isotherms on samples of attapulgite.

Table 1: The BET surface area, total pore volume, and average pore diameter of four NCMs.

Samples	BET surface area (m^2/g)	Total pore volume (cm^3/g)	Average pore diameter (nm)
Kaolinite	27.65	0.163	23.48
Zeolite	1.63	0.004	9.35
Attapulgite	92.91	0.133	5.71
Bentonite	47.78	0.046	3.83

3.2. Factors Affecting Adsorption

3.2.1. pH. The adsorption of ammonia nitrogen and phosphate on NCMs at different pH values was studied (Figure 5(a)). The results showed that the removal rate of attapulgite and bentonite for ammonia nitrogen was greater than that of kaolinite and zeolite, and the removal efficiency of NH_4^+ increased with pH from 2.0 to 6.0 and then decreased to 10.0. At lower pH (pH < 4.0), excess H^+ ions surpass the number of adsorption sites of NH_4^+ ions, reducing the removal efficiency of NH_4^+. The surface charge of the adsorbent is related to pH, and the H^+ concentration decreases with increasing pH, which weakens its competition for NCM particle adsorption/exchange sites, and the removal efficiency of NH_4^+ increased. As the pH increases from 6.0 to 10.0, the increase in anion binding sites can interact with NH_4^+, which further decreases the NH_4^+ concentration, greatly reducing the final adsorption capacity. The adsorption of phosphate is shown in Figure 5(d). At lower pH (pH < 4.0), the removal efficiency of PO_4^{3-} increases significantly and subsequently decreases slowly. Furthermore, under alkaline conditions, the higher concentration of OH^- in the solution enhances the competition between OH^- and phosphate on the surface of the adsorbent, thereby reducing phosphate adsorption [31, 49].

3.2.2. Adsorbent Dose. The adsorption of ammonia nitrogen and phosphate on NCMs under different adsorbent dosages was evaluated. As the adsorbent dosage increases from 0.1 g to 0.5 g, the removal efficiency of the four kinds of NCMs for NH_4^+ increases (Figure 5(b)). When the amount of adsorbents increases, the abundance of active sites available for adsorption increases accordingly, so the capacity of adsorbed ammonia nitrogen increases, thereby increasing the removal rate of ammonia nitrogen. However, the addition to the adsorption capacity of the four NCMs for ammonia nitrogen

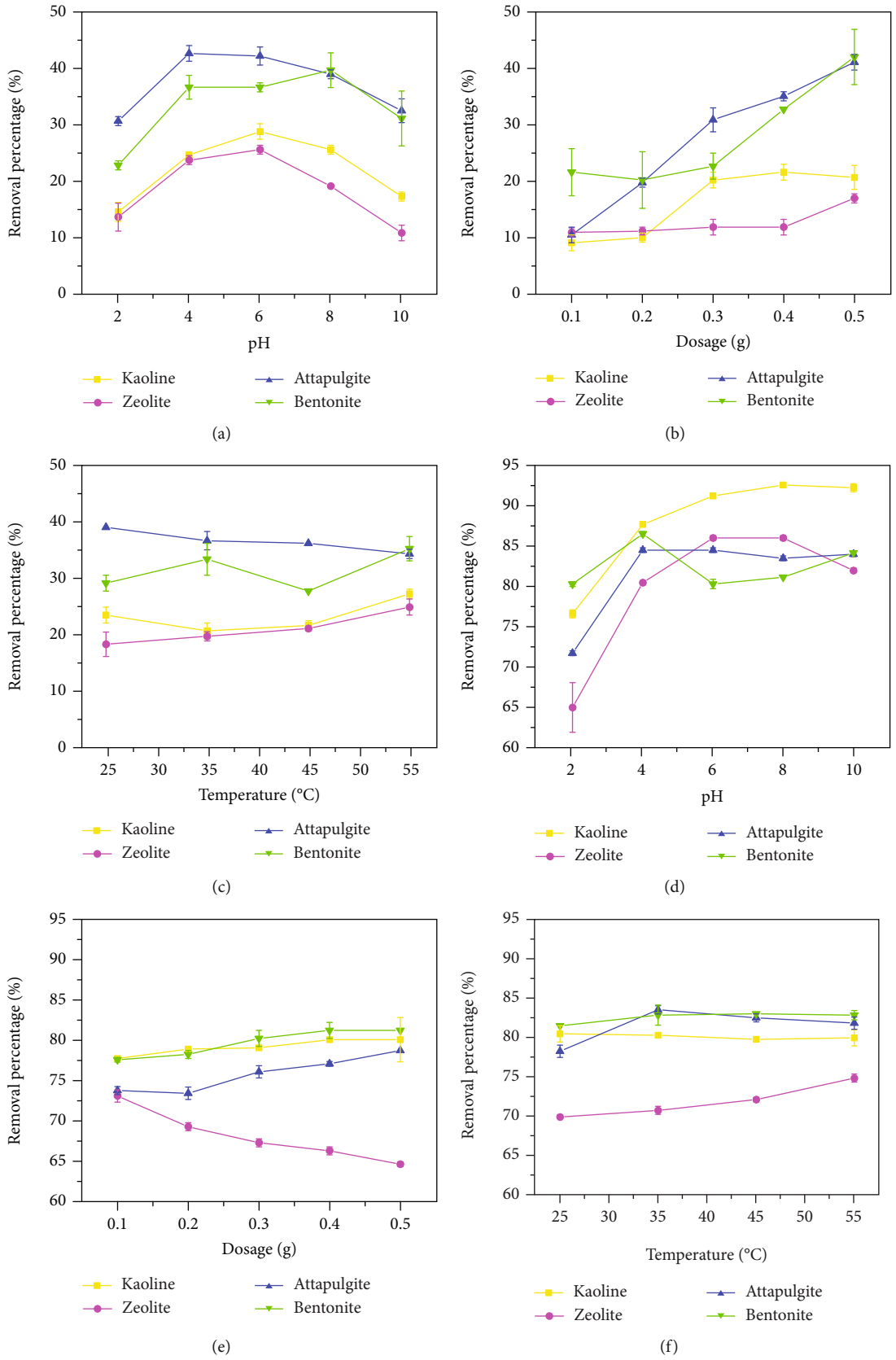

Figure 5: The removal rate of ammonia nitrogen (a–c) and phosphate (d–f) under different pH values, dosages, and temperatures.

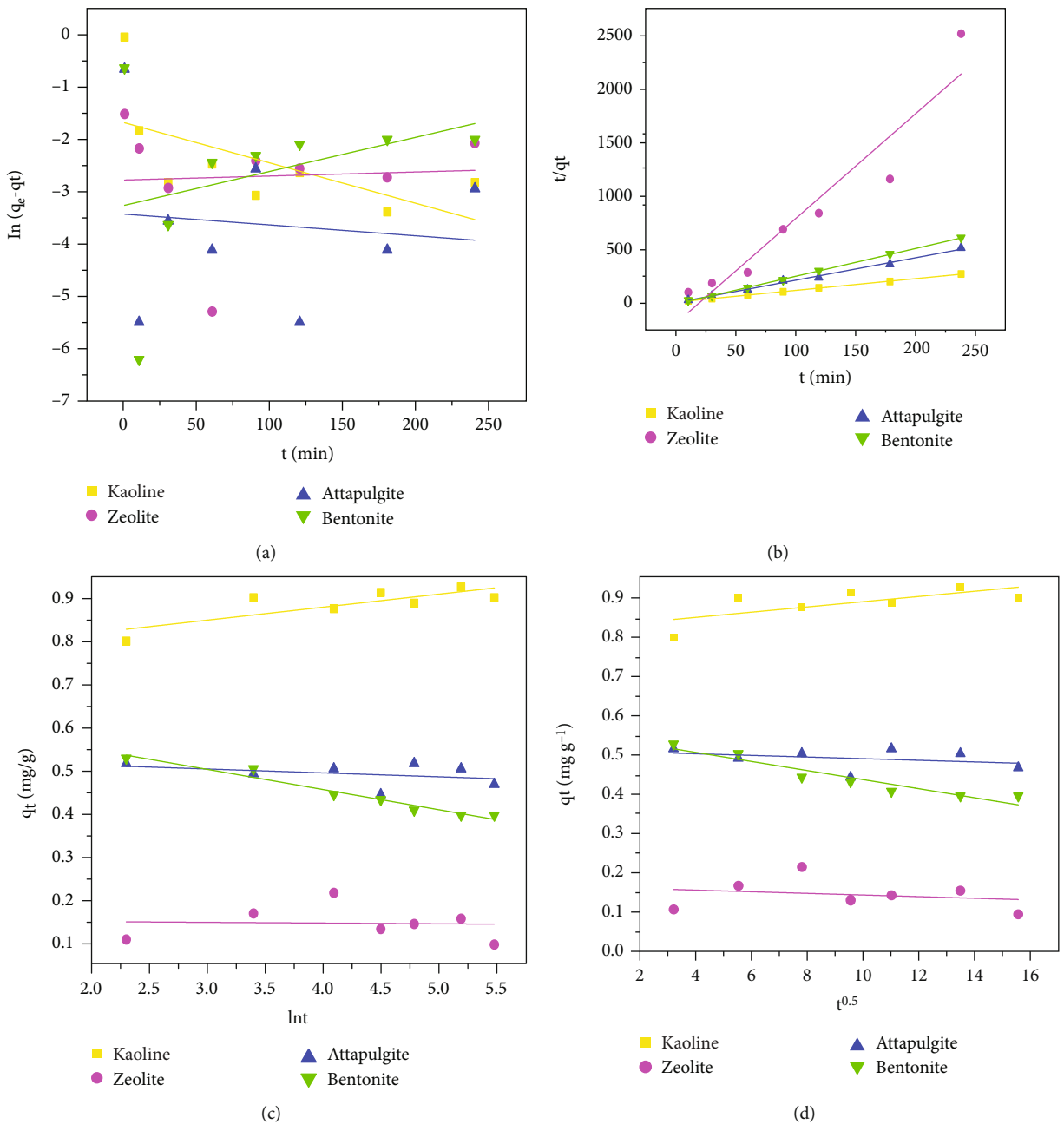

Figure 6: Four linear kinetic models for the adsorption of ammonia nitrogen on NCMs. (a) Pseudo-first-order kinetic model. (b) Pseudo-second-order kinetic model. (c) Elovich model. (d) Intraparticle diffusion model. $C_0 = 20\ \text{mg} \cdot \text{L}^{-1}$, $V = 25\ \text{mL}$, and temperature at 298 K.

is different. As shown in Figure 5(e), the adsorption of phosphate by the other three NCMs except zeolite increases with increasing adsorbent dosage. When the adsorbent dosage increases from 0.1 to 0.3 g, the adsorption is relatively rapid. This effect can be attributed to the increase in the specific surface area and available binding sites of the adsorbent [29]. With the increase in the amount of adsorbents, the available specific surface area increases, and the adsorption interaction between the two ions and the number of sites also increase, thereby increasing the overall removal efficiency, but the static unit volume of adsorbent dosage and adsorption capacity decrease. Generally, for a constant concentration of the target pollutant, increasing the adsorbent dose increases the number of contact points, thereby enhancing the adsorption of clay minerals. However, increasing the adsorbent dose to the peak results in decreased activity of the adsorbent on the specific surface area per unit volume, which in turn decreases the number of binding sites and reduces the removal rate [50].

3.2.3. Temperature. The adsorption of ammonia nitrogen and phosphate by four clay minerals at different temperatures was evaluated. As shown in Figure 5(c), the adsorption capacity of attapulgite and bentonite for ammonia nitrogen is greater than that of kaolinite and zeolite. As the temperature increases, the adsorption of attapulgite for ammonia

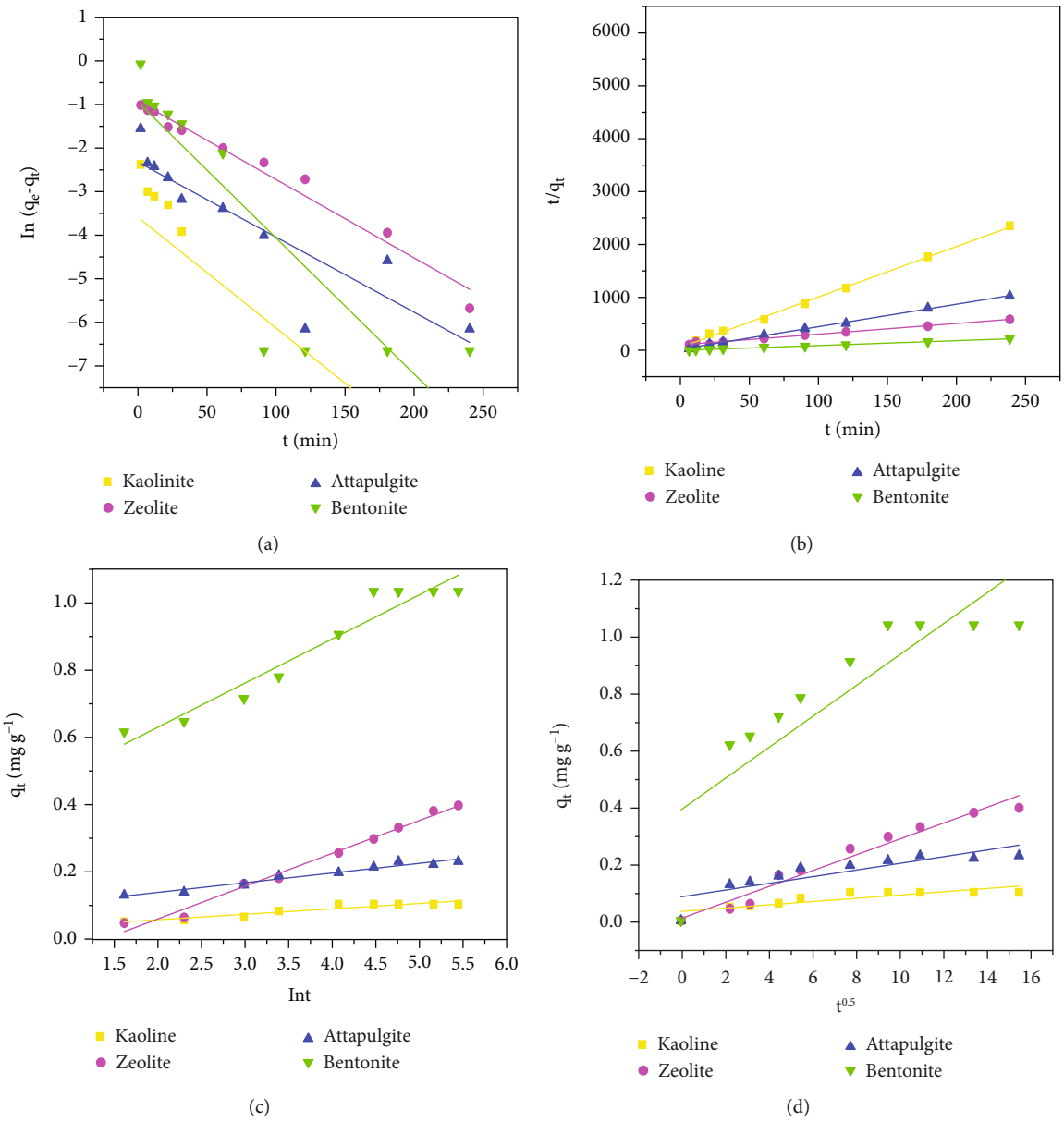

Figure 7: Four linear kinetic models for the adsorption of phosphate on NCMs. (a) Pseudo-first-order kinetic model. (b) Pseudo-second-order kinetic model. (c) Elovich model. (d) Intraparticle diffusion model. $C_0 = 10\,\text{mg} \cdot \text{L}^{-1}$, $V = 25\,\text{mL}$, and temperature at 298 K.

nitrogen decreases. As shown in Figure 5(f), with increasing temperature, the adsorption of phosphate by the four NCMs does not change significantly, indicating that the adsorption process does not have much influence in this temperature range. The adsorption of salt increases, but its removal capacity is lower than that of the other three NCMs. The removal efficiency of NH_4^+ decreases with increasing temperature, indicating that the adsorption of NH_4^+ is not affected by the increase in temperature and is exothermic during the adsorption process. The comparison temperature has almost no effect on the adsorption of PO_4^{3-}. It is possible that the different valence states of NH_4^+ and PO_4^{3-} lead to different changes in the surface charge and adsorption mechanism [38].

3.3. Adsorption Kinetic Analysis. The figures and correlation coefficients of the kinetic model are shown in Figures 6 and 7. The fitting effect of the pseudo-second-order kinetic model is good, and the correlation coefficient (R^2) values are all greater than 0.91, at approximately 0.99, except zeolite (Tables 2 and 3). In contrast, the correlation coefficient of the pseudo-first-order model is very low, much smaller than that of the pseudo-second-order model, indicating that the entire adsorption process is controlled by chemical adsorption, such as by ion sharing and transfer [51]. In addition, the match between the theoretical q_e value fitted by the pseudo-second-order kinetic model and the experimental q_e value illustrates the applicability of the pseudo-second-order equation in fitting the adsorption capacity.

Table 2: Linear form kinetic model parameters of ammonia nitrogen adsorption on NCMs.

Adsorbent type	Pseudo-first-order kinetic model			Pseudo-second-order kinetic model			Elovich model			Intraparticle diffusion model		
	q_e (mg/g)	K_1	R^2	q_e (mg/g)	K_2	R^2	a	b	R^2	C	K_{td}	R^2
Kaolinite	0.185	0.0078	0.3899	0.913	0.7360	0.9994	3805.7582	14.3802	0.6475	0.8245	0.0067	0.4876
Zeolite	0.062	-0.0008	0.0033	0.102	-0.0006	0.9109	-3.99*E*-20	-257.732	0.0021	0.1642	-0.0021	0.0504
Attapulgite	0.032	0.0021	0.0121	0.478	-0.1417	0.9943	-1.93*E*-13	-47.8928	0.1380	0.5115	-0.0021	0.1129
Bentonite	0.038	-0.0066	0.1128	0.386	-0.0236	0.9993	-0.000281	-9.2541	0.9557	0.5526	-0.0116	0.8999

Table 3: Linear form kinetic model parameters of phosphate adsorption on NCMs.

Adsorbent type	Pseudo-first-order kinetic model			Pseudo-second-order kinetic model			Elovich model			Intraparticle diffusion model		
	q_e (mg/g)	K_1	R^2	q_e (mg/g)	K_2	R^2	a	b	R^2	C	K_{td}	R^2
Kaolinite	0.0278	-0.0256	0.6536	0.1041	1.2218	0.9981	61.9963	0.0570	0.8958	0.0322	0.0057	0.7476
Zeolite	0.4222	-0.0181	0.9746	0.4902	0.0365	0.9899	10.2449	0.0232	0.9308	0.0075	0.0279	0.9635
Attapulgite	0.1022	-0.0174	0.7931	0.2335	0.5406	0.9985	34.7222	0.4196	0.9572	0.0834	0.0117	0.7238
Bentonite	0.4020	-0.0315	0.7731	1.0789	0.1239	0.9986	7.6167	2.1775	0.9400	0.3893	0.0543	0.7226

The values obtained by the Elovich model indicate that diffusion may be part of the rate-determining step, confirming that chemical adsorption may be part of the rate-limiting step [34].

Neither the pseudo-first-order equation nor the pseudo-second-order equation can explain the behavior of ammonia nitrogen and phosphate adsorption on natural clay minerals. Therefore, the intraparticle diffusion model was used to evaluate the diffusion mechanism and rate control steps that affect the adsorption kinetics of ammonia nitrogen [25]. The drawn intercept line of the intraparticle diffusion model cannot pass through the origin, indicating that although the intraparticle process of ammonia nitrogen and phosphate on natural clay minerals is a control step, it is not the only rate control step [52]. For simulation, the adsorption rate of natural clay minerals includes film diffusion, surface adsorption, and intraparticle diffusion for simulation [53].

3.4. Adsorption Isotherm Analysis. The adsorption isotherm of ammonia nitrogen was in good agreement with the Freundlich isotherm equilibrium model, and the adsorption isotherm of phosphate was in good agreement with the Langmuir II isotherm equilibrium model (Figure 8). Among all the NCMs studied, bentonite (7.13 mg/g) and kaolinite (5.37 mg/g) showed higher adsorption capacities for ammonia nitrogen, while zeolite (0.21 mg/g) and attapulgite (0.17 mg/g) showed higher adsorption capacities for phosphate.

The Freundlich model assumes that the surface of the adsorbent is not uniform and that there may be multiple layers of adsorption. The Freundlich model is more suitable for the adsorption isotherms of kaolinite and bentonite for ammonia nitrogen and fits the adsorption of phosphate by zeolite well ($R^2 > 0.99$). $1/n$ is the adsorption strength or surface unevenness, which represents the unevenness of the relative energy distribution and the position of the adsorbent [31]. When $1/n$ is greater than 0 ($0 < 1/n < 1$), adsorption is advantageous; when $1/n$ is greater than 1, the adsorption process is unfavorable; and when $1/n = 1$, the adsorption process is irreversible. Table 4 shows that kaolinite, attapulgite, and bentonite have $0 < 1/n < 1$, which is beneficial to the adsorption of ammonia nitrogen. The $1/n$ of zeolite is greater than 1, indicating that the adsorption of ammonia nitrogen by zeolite is unfavorable. Table 5 shows that kaolinite, zeolite, attapulgite, and bentonite have $0 < 1/n < 1$, indicating that these four clay minerals are all conducive to the adsorption of phosphate. The adsorption behavior of bentonite to phosphate is most in line with the Freundlich equation, indicating that the adsorption of phosphate by bentonite involves preferential adsorption, preferably multilayer adsorption, and that the adsorption process is more complicated [54]. The Temkin model has the well-fitting effect on the adsorption isotherms of the four clays' adsorption on ammonia nitrogen ($R^2 > 0.92$), indicating the multilayer adsorption occurs, and the nonideal multilayer chemical adsorption on uneven surfaces controls the adsorption process. The Temkin model assumes that the heat of adsorption decreases linearly with the adsorption capacity and is used to explain the chemical adsorption of heterogeneous surfaces [51].

Attapulgite is a hydrated aluminum-magnesium silicate mineral with a structure consisting of parallel ribbons of 2 : 1 layers. Natural zeolites are porous crystalline aluminosilicate minerals whose framework structure is negatively charged and can adsorb exchangeable cations such as Na^+, K^+, Ca^{2+}, and Mg^{2+} [55]. Some studies have found that Ca^{2+} in attapulgite can form a precipitate with PO_4^{3-} to achieve the effect of removing phosphate [56]. Kaolinite is a layered silicate clay mineral, and bentonite generally consists mostly of calcium montmorillonite, with permanent

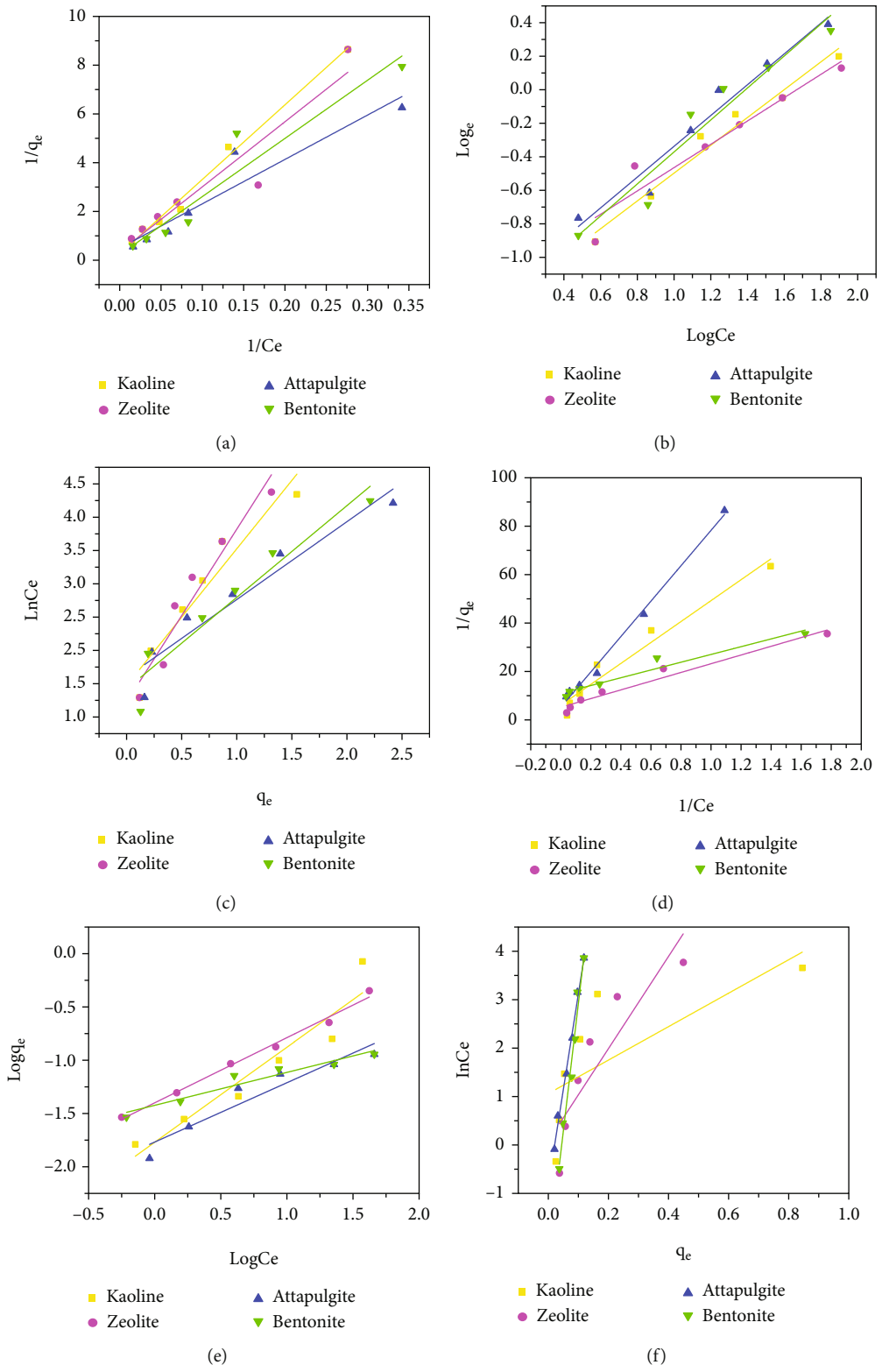

FIGURE 8: Three models for the adsorption of isotherms of NCMs on ammonia nitrogen ((a) Langmuir II model, (b) Freundlich model, and (c) Temkin model) and phosphate ((d) Langmuir II model, (e) Freundlich model, and (f) Temkin model). $V = 25$ mL, temperature at 298 K.

Table 4: Fitting results of the ammonia nitrogen adsorption isotherm.

Adsorbent type	Langmuir II			Freundlich			Temkin
	q_{max} (mg/g)	b (mg/L)	R^2	K_F	n	R^2	R^2
Kaolinite	5.37	0.1752	0.9918	0.0453	1.2070	0.9717	0.9249
Zeolite	3.74	0.1399	0.9019	0.0665	0.8900	0.9268	0.9318
Attapulgite	2.50	0.1371	0.9062	0.0537	1.0010	0.9586	0.9212
Bentonite	7.13	0.2982	0.9261	0.0458	1.4170	0.9352	0.9260

Table 5: Fitting results of the phosphate adsorption isotherm equation.

Adsorbent type	Langmuir II			Freundlich			Temkin
	q_{max} (mg/g)	b (mg/L)	R^2	K_F	n	R^2	R^2
Kaolinite	0.16	0.0038	0.9590	0.0165	0.8913	0.9084	0.5178
Zeolite	0.21	0.0117	0.9621	0.0389	0.6111	0.9915	0.7991
Attapulgite	0.17	0.0024	0.9939	0.0165	0.5562	0.9102	0.9915
Bentonite	0.09	0.0059	0.9517	0.0369	0.3089	0.9360	0.9717

negative charges on its interlamellar sites. To balance this negative charge, cations in water such as Ca^{2+}, Na^+, and Mg^{2+} are readily used as balance electrons, and it also gives ion exchangeability to bentonite [57]. The removal of NH_4^+ is the ion exchange of cations such as K^+, Mg^{2+}, and Na^+ for NH_4^+ in wastewaters [58].

4. Conclusion

Four NCM-based NH_4^+ and PO_4^{3-} adsorbents were studied and compared, and their adsorption behaviors were elucidated. Intermittent adsorption experiments show that the contact time, initial concentration, adsorbent dosage, and solution pH have significant effects on adsorption. Kinetic studies show that the adsorption process follows the pseudo-second-order kinetic model, and the adsorption isotherm is in good agreement with the Langmuir isotherm equilibrium model. In all NCMs studied, the adsorption capacity for ammonia nitrogen is bentonite>kaolinite>zeolite>attapulgite, and the adsorption capacity for phosphate is zeolite>attapulgite>kaolinite>bentonite. In particular, these four natural clay minerals have better adsorption effects on phosphate than on ammonia nitrogen and are more suitable for the treatment of phosphorus-containing wastewater. The use of NCMs reduces the treatment cost of nitrogen- and phosphorus-polluted water, with a certain reference value for NCMs in natural environment utilization. These research results provide a data reference for the prediction and evaluation of soil and lake eutrophication.

Data Availability

All data generated or analyzed during this study are included in this published article.

Additional Points

Highlights. (1) The adsorption of nitrogen and phosphorus by natural clay minerals (NCMs) was studied comprehensively. (2) The four NCMs had better adsorption efficiency for phosphate. (3) NCMs had application potential in removing nitrogen and phosphate in the natural water bodies or wastewater treatment.

Conflicts of Interest

The authors declared no potential conflicts of interest with respect to the research, authorship, and/or publication of this article.

Acknowledgments

The authors extend their appreciation to the support by the Open Research Fund of State Key Laboratory of Simulation and Regulation of Water Cycle in River Basin, China Institute of Water Resources and Hydropower Research (Grant No. IWHR-SKL-201907), China Energy Investment Corporation 2030 Pilot Project (Grant No. GJNY2030XDXM-19-03.2), National Key Research and Development Program of China (2020YFC1908601), National Natural Science Foundation of China (Grant No. 51878004), Anhui Provincial Outstanding Young Backbone Talents Visiting and Studying Program at Home and Abroad (Grant No. gxgwfx2019011), State Key Laboratory of Safety and Health for Metal Mines (Grant No. 2020-JSKSSYS-02), and Support Program for Excellent Talents in Universities of Anhui Province (Grant No. gxyqZD2021129). This study was also supported by the University Synergy Innovation Program of Anhui Province (Grant No. GXXT-2020-075). Thanks are due for the program from the Collaborative Innovation Center of Recovery and Reconstruction of Degraded Ecosystem in

Wanjiang Basin Co-founded by Anhui Province and Ministry of Education, Anhui Normal University, and State Key Laboratory of Safety and Health for Metal Mines, Sinosteel Maanshan General Institute of Mining Research Company Limited.

References

[1] Y. F. Wang, F. Lin, and W. Q. Pang, "Ammonium exchange in aqueous solution using Chinese natural clinoptilolite and modified zeolite," *Journal of Hazardous Materials*, vol. 142, no. 1-2, pp. 160–164, 2007.

[2] V. K. Gupta, S. Agarwal, and T. A. Saleh, "Synthesis and characterization of alumina-coated carbon nanotubes and their application for lead removal," *Journal of Hazardous Materials*, vol. 185, no. 1, pp. 17–23, 2011.

[3] M. Zamparas and I. Zacharias, "Restoration of eutrophic freshwater by managing internal nutrient loads. A review," *The Science of the Total Environment*, vol. 496, pp. 551–562, 2014.

[4] Q. Zeng, L. Qin, L. Bao, Y. Li, and X. Li, "Critical nutrient thresholds needed to control eutrophication and synergistic interactions between phosphorus and different nitrogen sources," *Environmental Science and Pollution Research*, vol. 23, no. 20, pp. 21008–21019, 2016.

[5] Q. Liu, Y. Zhang, H. Wu et al., "A review and perspective of eDNA application to eutrophication and HAB control in freshwater and marine ecosystems," *Microorganisms.*, vol. 8, no. 3, p. 417, 2020.

[6] Z. Sun, X. Qu, G. Wang, S. Zheng, and R. L. Frost, "Removal characteristics of ammonium nitrogen from wastewater by modified Ca- bentonites," *Applied Clay Science*, vol. 107, pp. 46–51, 2015.

[7] A. Gallego, L. Rodríguez, A. Hospido, M. T. Moreira, and G. Feijoo, "Development of regional characterization factors for aquatic eutrophication," *International Journal of Life Cycle Assessment*, vol. 15, no. 1, pp. 32–43, 2010.

[8] C. Le, Y. Zha, Y. Li, D. Sun, H. Lu, and B. Yin, "Eutrophication of lake waters in China: cost, causes, and control," *Environmental Management*, vol. 45, no. 4, pp. 662–668, 2010.

[9] Y. le Bagousse-Pinguet, P. Liancourt, N. Gross, and D. Straile, "Indirect facilitation promotes macrophyte survival and growth in freshwater ecosystems threatened by eutrophication," *Journal of Ecology*, vol. 100, no. 2, pp. 530–538, 2012.

[10] J. Huang, C.-C. Xu, B. G. Ridoutt, X. C. Wang, and P. A. Ren, "Nitrogen and phosphorus losses and eutrophication potential associated with fertilizer application to cropland in China," *Journal of Cleaner Production*, vol. 159, pp. 171–179, 2017.

[11] A. Mittal, J. Mittal, A. Malviya, D. Kaur, and V. K. Gupta, "Decoloration treatment of a hazardous triarylmethane dye, Light Green SF (Yellowish) by waste material adsorbents," *Journal of Colloid and Interface Science*, vol. 342, no. 2, pp. 518–527, 2010.

[12] O. Moradi, M. Yari, K. Zare, B. Mirza, and F. Najafi, "Carbon nanotubes: a review of chemistry principles and reactions," *Fullerenes, Nanotubes, and Carbon Nanostructures*, vol. 20, no. 2, pp. 138–151, 2012.

[13] H. P. Jarvie, A. N. Sharpley, P. J. A. Withers, J. T. Scott, B. E. Haggard, and C. Neal, "Phosphorus mitigation to control river eutrophication: murky waters, inconvenient truths, and "post-normal" science," *Journal of Environmental Quality*, vol. 42, no. 2, pp. 295–304, 2013.

[14] K. Vikrant, K.-H. Kim, Y. S. Ok et al., "Engineered/designer biochar for the removal of phosphate in water and wastewater," *The Science of the Total Environment*, vol. 616-617, pp. 1242–1260, 2018.

[15] G. Moussavi, S. Talebi, M. Farrokhi, and R. M. Sabouti, "The investigation of mechanism, kinetic and isotherm of ammonia and humic acid co-adsorption onto natural zeolite," *Chemical Engineering Journal*, vol. 171, no. 3, pp. 1159–1169, 2011.

[16] V. K. Gupta, S. K. Srivastava, D. Mohan, and S. Sharma, "Design parameters for fixed bed reactors of activated carbon developed from fertilizer waste for the removal of some heavy metal ions," *Waste Management*, vol. 17, no. 8, pp. 517–522, 1998.

[17] B. Cheknane, M. Baudu, J.-P. Basly, and O. Bouras, "Adsorption of basic dyes in single and mixture systems on granular inorganic-organic pillared clays," *Environmental Technology*, vol. 31, no. 7, pp. 815–822, 2010.

[18] R. Zhu, Q. Chen, Q. Zhou, Y. Xi, J. Zhu, and H. He, "Adsorbents based on montmorillonite for contaminant removal from water: a review," *Applied Clay Science*, vol. 123, pp. 239–258, 2016.

[19] F. Franco, M. Benítez-Guerrero, I. Gonzalez-Triviño et al., "Low-cost aluminum and iron oxides supported on dioctahedral and trioctahedral smectites: a comparative study of the effectiveness on the heavy metal adsorption from water," *Applied Clay Science*, vol. 119, pp. 321–332, 2016.

[20] D. Caputo and F. Pepe, "Experiments and data processing of ion exchange equilibria involving Italian natural zeolites: a review," *Microporous and Mesoporous Materials*, vol. 105, no. 3, pp. 222–231, 2007.

[21] W. L. Zhu, L. H. Cui, Y. Ouyang, C. F. Long, and X. D. Tang, "Kinetic adsorption of ammonium nitrogen by substrate materials for constructed wetlands," *Pedosphere*, vol. 21, no. 4, pp. 454–463, 2011.

[22] Y. Zhang, Y. Li, J. Li, L. Hu, and X. Zheng, "Enhanced removal of nitrate by a novel composite: nanoscale zero valent iron supported on pillared clay," *Chemical Engineering Journal*, vol. 171, no. 2, pp. 526–531, 2011.

[23] Y. Zhan, H. Zhang, J. Lin, Z. Zhang, and J. Gao, "Role of zeolite's exchangeable cations in phosphate adsorption onto zirconium- modified zeolite," *Journal of Molecular Liquids*, vol. 243, pp. 624–637, 2017.

[24] H. Cheng, Q. Zhu, and Z. Xing, "Adsorption of ammonia nitrogen in low temperature domestic wastewater by modification bentonite," *Journal of Cleaner Production*, vol. 233, pp. 720–730, 2019.

[25] A. Q. Selim, L. Sellaoui, and M. Mobarak, "Statistical physics modeling of phosphate adsorption onto chemically modified carbonaceous clay," *Journal of Molecular Liquids*, vol. 279, pp. 94–107, 2019.

[26] A. Kumar and P. Lingfa, "Sodium bentonite and kaolin clays: comparative study on their FT-IR, XRF, and XRD," *Materials Today: Proceedings.*, vol. 22, pp. 737–742, 2020.

[27] C. Xiong, D. Wang, N. F. Tam et al., "Enhancement of active thin-layer capping with natural zeolite to simultaneously inhibit nutrient and heavy metal release from sediments," *Ecological Engineering*, vol. 119, pp. 64–72, 2018.

[28] D. Copetti, K. Finsterle, L. Marziali et al., "Eutrophication management in surface waters using lanthanum modified

bentonite: a review," *Water Research*, vol. 97, pp. 162–174, 2016.

[29] A. Alshameri, C. Yan, and X. Lei, "Enhancement of phosphate removal from water by TiO_2/Yemeni natural zeolite: preparation, characterization and thermodynamic," *Microporous and Mesoporous Materials*, vol. 196, pp. 145–157, 2014.

[30] M. Zamparas, M. Drosos, Y. Georgiou, Y. Deligiannakis, and I. Zacharias, "A novel bentonite-humic acid composite material Bephos™ for removal of phosphate and ammonium from eutrophic waters," *Chemical Engineering Journal*, vol. 225, pp. 43–51, 2013.

[31] Q. X. Jing, L. Y. Chai, X. D. Huang, C. J. Tang, H. Guo, and W. Wang, "Behavior of ammonium adsorption by clay mineral halloysite," *Transactions of Nonferrous Metals Society of China*, vol. 27, no. 7, pp. 1627–1635, 2017.

[32] B.-W. Gu, S.-H. Hong, C.-G. Lee, and S. J. Park, "The feasibility of using bentonite, illite, and zeolite as capping materials to stabilize nutrients and interrupt their release from contaminated lake sediments," *Chemosphere*, vol. 219, pp. 217–226, 2019.

[33] M. K. Seliem, S. Komarneni, T. Byrne et al., "Removal of perchlorate by synthetic organosilicas and organoclay: kinetics and isotherm studies," *Applied Clay Science*, vol. 71, pp. 21–26, 2013.

[34] G. Li, W. Zhu, C. Zhang et al., "Effect of a magnetic field on the adsorptive removal of methylene blue onto wheat straw biochar," *Bioresource Technology*, vol. 206, pp. 16–22, 2016.

[35] W. J. Weber Jr. and J. C. Morris, "Kinetics of adsorption on carbon from solution," *Journal of the Sanitary Engineering Division*, vol. 89, no. 2, pp. 31–59, 1963.

[36] Y. S. Ho and G. McKay, "Sorption of dye from aqueous solution by peat," *Chemical Engineering Journal*, vol. 70, no. 2, pp. 115–124, 1998.

[37] Y. S. Ho and G. McKay, "Pseudo-second order model for sorption processes," *Process Biochemistry*, vol. 34, no. 5, pp. 451–465, 1999.

[38] C. W. Cheung, J. F. Porter, and G. McKay, "Sorption kinetics for the removal of copper and zinc from effluents using bone char," *Separation and Purification Technology*, vol. 19, no. 1-2, pp. 55–64, 2000.

[39] L. Zheng, Y. Yang, P. Meng, and D. Peng, "Absorption of cadmium (II) via sulfur-chelating based cellulose: characterization, isotherm models and their error analysis," *Carbohydrate Polymers*, vol. 209, pp. 38–50, 2019.

[40] A. Alshameri, H. He, J. Zhu et al., "Adsorption of ammonium by different natural clay minerals: characterization, kinetics and adsorption isotherms," *Applied Clay Science*, vol. 159, pp. 83–93, 2018.

[41] M. Doumeng, L. Makhlouf, F. Berthet et al., "A comparative study of the crystallinity of polyetheretherketone by using density, DSC, XRD, and Raman spectroscopy techniques," *Polymer Testing*, vol. 93, article 106878, 2021.

[42] X. Zhang, S. Lin, Z. Chen, M. Megharaj, and R. Naidu, "Kaolinite-supported nanoscale zero-valent iron for removal of Pb^{2+} from aqueous solution: reactivity, characterization and mechanism," *Water Research*, vol. 45, no. 11, pp. 3481–3488, 2011.

[43] M. Saifuddin, J. Bae, and K. S. Kim, "Role of Fe, Na and Al in Fe-zeolite-A for adsorption and desorption of phosphate from aqueous solution," *Water Research*, vol. 158, pp. 246–256, 2019.

[44] R. Huang, Q. Lin, Q. Zhong, X. Zhang, X. Wen, and H. Luo, "Removal of Cd(II) and Pb(II) from aqueous solution by modified attapulgite clay," *Arabian Journal of Chemistry*, vol. 13, no. 4, pp. 4994–5008, 2020.

[45] J. Wang, D. Zhang, S. Liu, and C. Wang, "Enhanced removal of chromium(III) for aqueous solution by EDTA modified attapulgite: adsorption performance and mechanism," *Science of The Total Environment.*, vol. 720, article 137391, 2020.

[46] A. M. Ahmat, T. Thiebault, and R. Guégan, "Phenolic acids interactions with clay minerals: a spotlight on the adsorption mechanisms of gallic acid onto montmorillonite," *Applied Clay Science*, vol. 180, article 105188, 2019.

[47] A. B. Rakhym, G. A. Seilkhanova, and T. S. Kurmanbayeva, "Adsorption of lead (II) ions from water solutions with natural zeolite and chamotte clay," *Materials Today: Proceedings.*, vol. 31, pp. 482–485, 2020.

[48] R. A. Schoonheydt, "Reflections on the material science of clay minerals," *Applied Clay Science*, vol. 131, pp. 107–112, 2016.

[49] F. Gérard, "Clay minerals, iron/aluminum oxides, and their contribution to phosphate sorption in soils – A myth revisited," *Geoderma*, vol. 262, pp. 213–226, 2016.

[50] Q. Xu, W. Li, L. Ma, D. Cao, G. Owens, and Z. Chen, "Simultaneous removal of ammonia and phosphate using green synthesized iron oxide nanoparticles dispersed onto zeolite," *Science of The Total Environment.*, vol. 703, article 135002, 2020.

[51] H. Ge, C. Wang, S. Liu, and Z. Huang, "Synthesis of citric acid functionalized magnetic graphene oxide coated corn straw for methylene blue adsorption," *Bioresource Technology*, vol. 221, pp. 419–429, 2016.

[52] M. Arami, N. Y. Limaee, and N. M. Mahmoodi, "Evaluation of the adsorption kinetics and equilibrium for the potential removal of acid dyes using a biosorbent," *Chemical Engineering Journal*, vol. 139, no. 1, pp. 2–10, 2008.

[53] W. Huang, J. Chen, and J. Zhang, "Adsorption characteristics of methylene blue by biochar prepared using sheep, rabbit and pig manure," *Environmental Science and Pollution Research*, vol. 25, no. 29, pp. 29256–29266, 2018.

[54] Y. Dehmani, L. Sellaoui, Y. Alghamdi et al., "Kinetic, thermodynamic and mechanism study of the adsorption of phenol on Moroccan clay," *Journal of Molecular Liquids*, vol. 312, article 113383, 2020.

[55] D. Guaya, C. Valderrama, A. Farran, C. Armijos, and J. L. Cortina, "Simultaneous phosphate and ammonium removal from aqueous solution by a hydrated aluminum oxide modified natural zeolite," *Chemical Engineering Journal*, vol. 271, pp. 204–213, 2015.

[56] H. Yin and M. Kong, "Simultaneous removal of ammonium and phosphate from eutrophic waters using natural calcium-rich attapulgite-based versatile adsorbent," *Desalination*, vol. 351, pp. 128–137, 2014.

[57] L. Gu, J. Xu, L. Lv et al., "Dissolved organic nitrogen (DON) adsorption by using Al-pillared bentonite," *Desalination*, vol. 269, no. 1-3, pp. 206–213, 2011.

[58] N. Karapınar, "Application of natural zeolite for phosphorus and ammonium removal from aqueous solutions," *Journal of Hazardous Materials*, vol. 170, no. 2-3, pp. 1186–1191, 2009.